Cardiovascular Research (2015) **106**, 421–431
doi:10.1093/cvr/cvv128

Deriving a cardiac ageing signature to reveal MMP-9-dependent inflammatory signalling in senescence

Yonggang Ma[1,2†], Ying Ann Chiao[1,3†], Ryan Clark[1,2], Elizabeth R. Flynn[1,2], Andriy Yabluchanskiy[1,2], Omid Ghasemi[1,4], Fouad Zouein[1,2], Merry L. Lindsey[1,2,5*], and Yu-Fang Jin[1,4*]

[1]San Antonio Cardiovascular Proteomics Center, San Antonio, TX 78229, USA; [2]Mississippi Center for Heart Research, Department of Physiology and Biophysics, University of Mississippi Medical Center, 2500 North State St., Jackson, MS 39216-4505, USA; [3]Department of Pathology, University of Washington, Seattle, WA, USA; [4]Department of Electrical and Computer Engineering, The University of Texas at San Antonio, One UTSA Circle, San Antonio, TX 78249, USA; and [5]Research Services, G.V. (Sonny) Montgomery Veterans Affairs Medical Center, Jackson, MS, USA

Received 5 October 2014; revised 29 March 2015; accepted 2 April 2015; online publish-ahead-of-print 15 April 2015

Time for primary review: 34 days

Aims Cardiac ageing involves the progressive development of cardiac fibrosis and diastolic dysfunction coordinated by MMP-9. Here, we report a cardiac ageing signature that encompasses macrophage pro-inflammatory signalling in the left ventricle (LV) and distinguishes biological from chronological ageing.

Methods and results Young (6–9 months), middle-aged (12–15 months), old (18–24 months), and senescent (26–34 months) mice of both C57BL/6J wild type (WT) and MMP-9 null were evaluated. Using an identified inflammatory pattern, we were able to define individual mice based on their biological, rather than chronological, age. *Bcl6*, *Ccl24*, and *Il4* were the strongest inflammatory markers of the cardiac ageing signature. The decline in early-to-late LV filling ratio was most strongly predicted by *Bcl6*, *Il1r1*, *Ccl24*, *Crp*, and *Cxcl13* patterns, whereas LV wall thickness was most predicted by *Abcf1*, *Tollip*, *Scye1*, and *Mif* patterns. With age, there was a linear increase in cardiac M1 macrophages and a decrease in cardiac M2 macrophages in WT mice; of which, both were prevented by MMP-9 deletion. *In vitro*, MMP-9 directly activated young macrophage polarization to an M1/M2 mid-transition state.

Conclusion Our results define the cardiac ageing inflammatory signature and assign MMP-9 roles in mediating the inflammaging profile by indirectly and directly modifying macrophage polarization. Our results explain early mechanisms that stimulate ageing-induced cardiac fibrosis and diastolic dysfunction.

Keywords Cardiac ageing • Inflammation • Macrophage polarization • MMP-9 • Proteomics

1. Introduction

Cardiac ageing is a major risk factor that dramatically increases cardiovascular disease morbidity and mortality.[1] While ageing is a risk factor for the population as an average, understanding ageing at the individual level remains a challenge. Chronological age is defined as the actual age (number of years an individual has lived). Biological age is defined as the phenotypic age of the individual compared with the average phenotype for the population. Biological age can be calculated by measuring factors with the largest influence on longevity and comparing the individual values to the group mean. While Weale and colleagues[2] have proposed a system for evaluating biological age, this system is a global assessment and not specific for the heart.

We and others have previously shown that cardiac ageing leads to impaired diastolic function of the left ventricle (LV), due to the development of cardiac muscle sarcopenia characterized by cardiomyocyte loss and collagen accumulation.[3–5] While our knowledge of the molecular basis responsible for these alterations remains limited, a common mediator of ageing is increased inflammation (inflammaging).

Inflammaging is characterized by the increase in inflammatory cytokines over the course of ageing and is believed to play a critical role in ageing-induced cardiac remodelling.[6] Plasma monocyte chemotactic

* Corresponding author. Tel: +1 601 815 1329; fax: +1 601 984 1817, Email: mllindsey@umc.edu (M.L.L.); Tel: +1 210 458 5588; fax: +1 210 458 5947, Email: yufang.jin@utsa.edu (Y.-F.J.)
† Co-first authors.

protein-1 (MCP-1) and MMP-9 increase with age, and both positively correlate with the increase in end-diastolic dimensions.[7] MCP-1, also known as Ccl2, is a potent CC chemokine that recruits monocytes to the sites of inflammation or injury.[8] We have demonstrated that macrophages increase in the LV of senescent (26–34 months) mice and contribute to the increase in MMP-9 with age.[7] Atorvastatin delays cardiac ageing in rats by reducing IL-1β, TNF-α, and MMP-9.[9] Caloric restriction in humans induces a younger transcription profile that is also associated with a diminished inflammatory pattern.[10] Combined, these past reports from our group and others provide substantial support for the inflammatory hypothesis of cardiac ageing.

MMP-9 is involved in multiple cardiovascular diseases, including myocardial infarction. MMP-9 deletion attenuates post-MI LV remodelling and dysfunction by inhibiting macrophage infiltration, inflammatory and fibrotic responses, as well as facilitating angiogenesis.[11,12] MMP-9 deletion alleviates cardiac fibrosis and preserves LV diastolic function by modifying the extracellular matrix response and angiogenesis in aged mice.[5,13] The impact of MMP-9 deletion on the inflammatory reaction over the course of cardiac ageing, however, remains to be elucidated.

Based on the above background, we hypothesized that MMP-9 deletion would attenuate age-related LV diastolic dysfunction by regulating inflammation. Here, we established the cardiac inflammaging pattern in mice, to study the interplay between MMP-9 and macrophages over the lifespan. We discovered that the biological ageing signature could be distinguished from chronological age. We propose a model of cardiac ageing mediated by MMP-9 effects on macrophage polarization, with this signature linking to LV structure and function.

2. Methods

2.1 Mice

All animal procedures were conducted in accordance with the Guide for the Care and Use of Laboratory Animals and were approved by the Institutional Animal Care and Use Committee at the University of Texas Health Science Center at San Antonio and the University of Mississippi Medical Center.

The C57BL/6J wild-type (WT) and MMP-9 null young (6–9 months), middle-aged (MA; 12–15 months), old (18–24 months), and senescent (26–34 months) mice of both sexes were evaluated ($n \geq 12$/group). MMP-9 null mice were a gift from Dr Zena Werb through Dr Lynn Matrisian, whose laboratory backcrossed the mice onto the C57BL/6J strain.[14,15] The mice and tissue used for this study were previously evaluated for extracellular matrix effects.[5] A new cohort of young, MA, old, and senescent mice of WT ($n = 21$) and MMP-9 null ($n = 18$) were used for flow cytometry and macrophage experiments. A cohort of 3- to 6-month-old male WT mice ($n = 8$) were used to isolate and stimulate peritoneal macrophages. Mice were euthanized with 5% isoflurane, followed by exsanguination and removal of the heart.

2.2 Quantitative inflammatory gene array

Total RNA was isolated from the LV base using TRIzol reagent (15596026, Life technologies) plus the Total RNA purification kit (12183018A, Life Technologies), and cDNA was synthesized using the SABiosciences RT^2 first strand kit (330401, Qiagen). To assess mRNA expression of inflammatory markers in the LV, the mouse inflammatory cytokines, and receptors, PCR array (PAMM-011A, Qiagen) was used.[16] We followed the MIQE guidelines for PCR experiments and analysis.[17] Our previous studies demonstrated that several of the measured reference genes (*Gusb*, *Hsp90ab1*, *Gapdh*, and *Actb*), but not *Hprt1*, changed and could not be used for normalization. Therefore, in this study, we used only *Hprt1*, instead of all five reference genes, to normalize the threshold cycle (C_t) values of individual target genes. The $2^{-\Delta C_t} \times 100$ values were used for statistical and biclustering analyses. A total of $n = 6$ samples per group were used.

2.3 Biclustering analysis

A total of 35 genes were statistically different between WT and MMP-9 null mice (*Table 1*). The young mice served as control groups and expression levels of genes in MA, old, and senescent mice were normalized to respective young controls for fold changes. We applied a biclustering algorithm to examine the fold changes.[18] Average fold changes of the 35 genes were clustered to have the biological ageing signature as shown in *Figure 1*.

2.4 LV wall thickness measurement

LV wall thickness in diastole was measured from two-dimensional M-mode echocardiographic images using the Vevo770 software. For each mouse, three independent measurements were made and averaged.

2.5 Immunoblotting

The protein was extracted by homogenizing the samples in protein extraction reagent type 4 (C0356, Sigma-Aldrich). Protein concentrations were determined using the Quick Start™ Bradford Protein Assay (500–0205, Bio-Rad). Protein expression levels of Bcl6 (ab19011, Abcam) and IL-4 (ab11524, Abcam) were quantified by immunoblot, as reported previously.[16,19] The relative expression for each immunoblot was calculated as the densitometry of the protein of interest divided by the densitometry of the entire lane of the total protein stained membrane.

2.6 Macrophage immunohistochemistry

Immunohistochemistry for Mac-3 (CL8493AP, Cedarlane) was performed on the mid LV section to measure macrophage accumulation. Paraffin-embedded LV sections were deparaffinized in CitriSolve (22-143-975, Fisher Scientific) and rehydrated by incubating twice in 100, 95, and 70% ethanol, and distilled water for 5 min each. After heat-mediated antigen retrieval was performed using the Target Retrieval Solution (S1699, Dako), the sections were incubated in 3% hydrogen peroxide (216763, Sigma) to quench endogenous peroxidase activity. The sections were blocked with rabbit normal serum and incubated with an anti-Mac-3 antibody, followed by incubation with rabbit anti-rat IgG and ABC reagent (PK-6104, Vector Laboratories). HistoMark Black Peroxidase Substrate Kit (54-75-00, KPL) was used for colour development. The sections were counterstained with eosin, dehydrated, and mounted. Quantification was calculated as the percentage of positive stained area to the total area. Previously, we showed increased macrophage numbers in senescent (26–34 months) LV, compared with young mice ($n = 3$/group).[7] In the current study, we expanded the sample size to $n = 9$–13/group.

2.7 Cardiac macrophage isolation

The LV was minced and dissociated into single cell suspension with a cocktail of collagenase II and DNase I, as described previously.[20] The cell suspension was applied over pre-separation filters (130-041-407, Miltenyi Biotec) to remove non-dissociated clumps and incubated with red blood cell lysis solution (130-094-183, Miltenyi Biotec) to remove red blood cells. The single cell suspension was incubated with anti-Ly-6G-Biotin and anti-Biotin Microbeads (130-092-332, Miltenyi Biotec). The cell suspension was applied over a magnetic MS column (130-042-201, Miltenyi Biotec) and Ly-6G$^+$ neutrophils adhered to columns. The flowthrough (Ly-6G$^-$ cells) was incubated with CD11b Microbeads (130-049-601, Miltenyi Biotec). The cell suspension was applied over a magnetic MS column. The neutrophil-depleted CD11b$^+$ cells (macrophages) were collected.[20] Two mice were pooled to acquire enough macrophage numbers for each sample set, and a minimum of $n = 3$ sets were used for each group.

2.8 Peritoneal macrophage isolation

To isolate peritoneal macrophages, 10 mL of ice-cold RPMI1640 media (11875093, Life technologies) with 10% fetal bovine serum (FBS 16000, Life Technologies) and 1% antibiotics (15240, Life Technologies) was injected into the peritoneal cavity of mice that had been overdosed with isoflurane. After 5 min of incubation, media was withdrawn from the peritoneal cavity and stored on ice. Another 10 mL of ice-cold RPMI1640 media was injected and subsequently withdrawn from the peritoneal cavity. The collected media was centrifuged at 1000 × *g* for 10 min. The cell pellet was resuspended in 5 mL of RPMI1640 media, and the cells were plated in a six-well plate (1×10^6 cells/well) and incubated at 37°C to allow the cells to adhere. After 5 h, the media was discarded, and the wells were washed with 1× phosphate-buffered saline to remove non-adherent cells.[16,20]

2.9 Flow cytometry for evaluating macrophage phenotype

The single cell suspension or isolated peritoneal macrophages were blocked with 5% heat-inactivated mouse serum and incubated with an APC anti-mouse F4/80 antibody (123116, Biolegend) and Alexa Fluor® 488 anti-CD206 antibody (MCA2235A488T, AbD Serotec). The unstained cells and/or cells stained with isotype-matched IgG were used as negative controls. The flow cytometry experiments were performed using a MACSQuant® Analyzer 10 and the data analysed by the MACSQuantify™ software. Macrophages from both cardiac and peritoneal sources were defined as $F4/80^+CD206^-$ for M1 or $F4/80^+CD206^+$ for M2, as reported by others.[21]

2.10 Macrophage stimulation

Isolated peritoneal macrophages were stimulated with 0.5 μg/mL of recombinant human active MMP-9 (PF140, Millipore) for 4 h. The cells were harvested for evaluating macrophage phenotype by real-time PCR.

2.11 Real-time PCR for macrophage M1 and M2 markers

Total RNA was isolated from peritoneal macrophages and LVs, and cDNA was synthesized as described before.[19] The expression levels of M1 markers *Ccl3* (Mm00441259_g1), *Ccl5*, (Mm01302427_m1), *Il1b* (Mm01336189_m1), *Il6* (Mm00843434_s1), *Pf4* (Mm00451315_g1), *Tnfα* (Mm00443258_m1), as well as M2 markers *Arg1* (Mm00475988_m1), *Cd163* (Mm00474091_m1), *Cd206* (Mm00485148_m1), *Fizz1* (Mm00445109_m1), *Il10* (Mm00439614_m1), *Tgfb1* (Mm01178820_m1), and *Ym1* (Mm00657889_mH) were measured with Taqman gene expression assay, with *Hprt1* (Mm01545399_m1) as the reference gene. The $2^{-\Delta C_t}$ values were expressed as fold change, normalized to WT young mice in *Figure 4B*, or unstimulated cells in *Figure 4C* and Supplementary material online, *Figure S2*.

2.12 Statistical analysis

Data are expressed as mean ± SEM. Two- or one-way ANOVA with appropriate post-test was used to compare values among groups. Pearson correlation was performed to determine correlation coefficients. Comparisons between two groups were carried out using Student's *t*-test. A value of $P < 0.05$ was considered statistically significant. STATA version 11 and GraphPad Prism 6 were used for the statistical analyses.

3. Results

3.1 MMP-9 regulated ageing-associated inflammation

To investigate the effect of age and MMP-9 on cardiac inflammation, we performed gene array for 84 inflammatory factors in young, MA, old, and senescent (26–34 months) LVs of WT and MMP-9 null mice (see Supplementary material online, *Table S1*). There were 35 genes statistically different among groups analysed by two-way ANOVA, and these genes are listed in *Table 1*. Of those, 16 genes demonstrated ageing-dependent changes in WT (*Table 1*, left column). MMP-9 deletion removed 10 of those changes (6 were different in both WT and MMP-9 null) and added in 15 new genes, for a total of 21 genes changed with age in the absence of MMP-9 (*Table 1, right column*). This indicated a strong dependence of cardiac ageing on MMP-9. The six genes in common between WT and MMP-9 null were *Abcf1*, *Ccr7*, *Il6st*, *Mif*, *Scye1*, and *Tollip*. There were 10 genes (*Casp1*, *Ccl5*, *Ccl7*, *Ccr2*, *Cd40lg*, *Cxcl9*, *Cxcl10*, *Cxcr3*, *Ifng*, and *Xcr1*) differentially altered between WT and MMP-9 null young mice (see Supplementary material online, *Table S1*).

Table 1 Inflammatory gene array results for WT and MMP-9 null mice

WT ageing-dependent	MMP-9 null ageing-dependent
Abcf1	Abcf1
Bcl6	–
–	Ccl2
–	Ccl4
–	Cc7
Ccl19	–
Ccl24	–
Ccr7	Ccr7
CCr9	–
–	Crp
–	Cxcl1
–	Cxcl9
–	Cxcl10
Cxcl13	–
–	Cxcr3
–	Ifng
–	Il1r1
–	Il2rg
Il4	–
Il6st	Il6st
–	Il8rb
Il10	–
Il13	–
–	Il15
Il16	–
Mif	Mif
Scye1	Scye1
Spp1	–
–	Tnf
Tollip	Tollip
–	Xcr1

Out of 84 genes, 35 genes were statistically different among groups. WT showed 16 genes and MMP-9 null showed 21 genes that were age-dependent, of which six were in common (*Abcf1*, *Ccr7*, *Il6st*, *Mif*, *Scye1*, and *Tollip*). See also Supplementary material online, *Table S1*.

3.2 Reducing pattern complexity to identify the most significant differences

The 35 genes that showed strong differences with age or MMP-9 deletion were normalized to respective young controls and analysed with a biclustering algorithm. The algorithm grouped patterns of change to

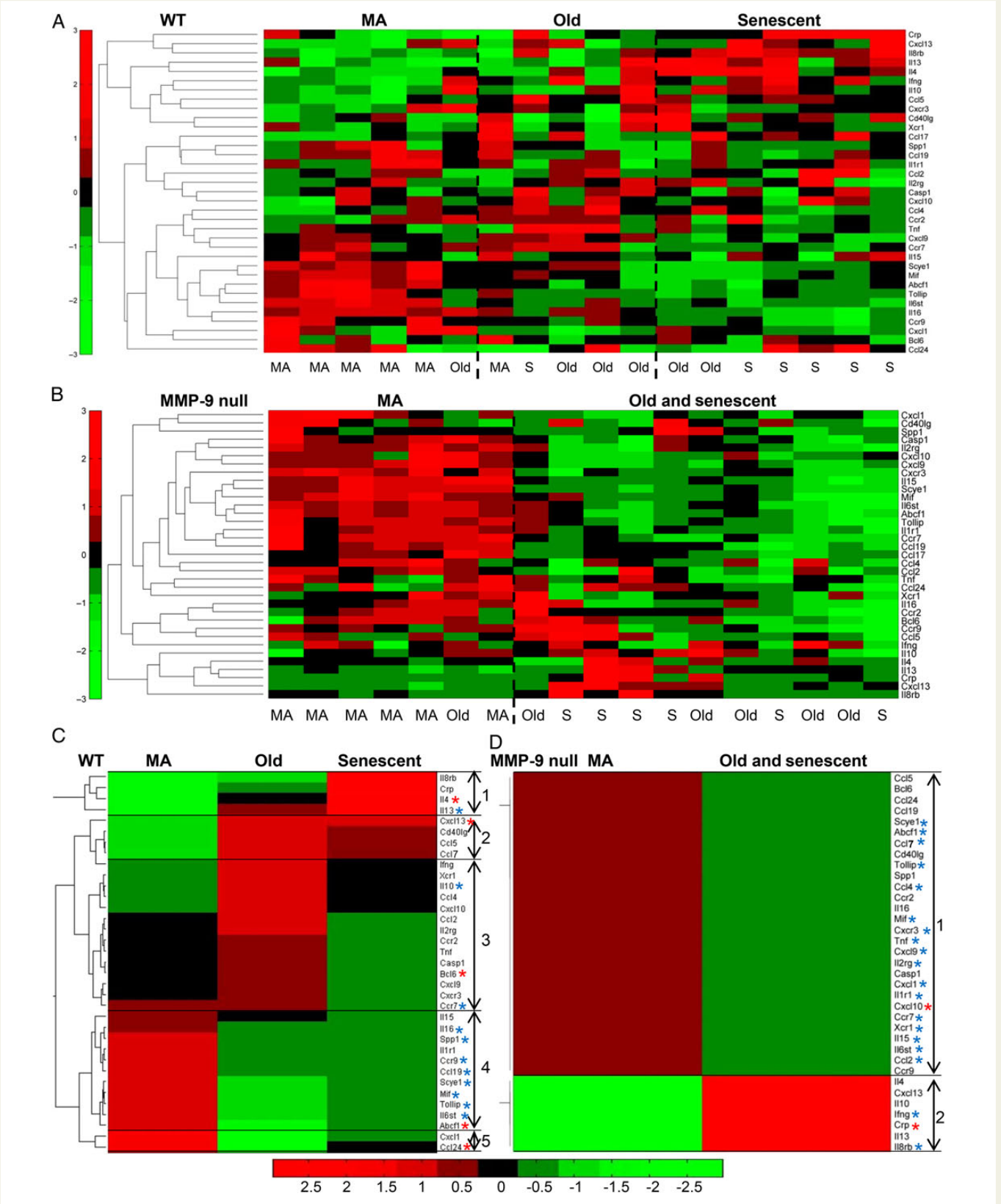

Figure 1 Pattern of inflammation with age revealed by biclustering algorithm. (*A*) Biological age classification for WT mice. (*B*) Biological age classification for MMP-9 null mice. (*C* and *D*) A biclustering algorithm showed a change pattern of inflammation with biological age and with MMP-9 deletion. Gene expression levels in middle-aged (MA), old, and senescent (S, 26–34 months) mice were normalized to respective young controls. Only genes that were significantly different in either WT or MMP-9 null for biclustering algorithm are listed here ($n = 35$ genes). In the colour legend, red represents up-regulation of genes with respect to the young control and green represents down-regulation of genes with respect to the young control; asterisks denote WT ageing-dependent or MMP-9 null ageing-dependent, with red highlighted being the markers that best represented the configuration. $n = 6$/group.

evaluate biological (vs. chronological) age, and the individual biological replicates are shown in *Figure 1A* and *B*. The algorithm revealed three patterns of change for WT (*Figure 1C*), indicating that WT mice could be separated biologically into MA, old, and senescent groups. Of note, the MMP-9 null group could only be separated into two groups (MA and old/senescent groups, *Figure 1D*), indicating that biological ageing was slowed in the absence of MMP-9.

For the MA pattern of the WT (MA biological age), five MA and one old were grouped together, indicating that one old mouse showed a younger biological phenotype than its chronological age. This pattern was termed the MA biological ageing pattern (*Figure 1A* and *C*). The second pattern (old biological age) contained one MA, three old, and one senescent, indicating that one MA mouse was older than its age and one senescent mouse was younger than its age. The third group was termed the senescent biological pattern, which included two old and five senescent, indicating that two old mice were older than their age. These patterns indicated a divergence between chronological age based on actual age and biological age based on gene profiles.

In the MMP-9 null, the first pattern contained six MA and one old, indicating that one old MMP-9 null mouse showed a younger biological phenotype than its chronological age. The second old and senescent pattern contained five old and six senescent (*Figure 1B* and *D*), indicating that all senescent MMP-9 null mice were biologically younger than their chronological age.

There were five configurations in the WT that defined the cardiac ageing pattern (*Figure 1C*). The first configuration was down-regulated in MA, gradually increased in old, and was up-regulated in senescence. This configuration contained four genes (*Il8rb*, *Crp*, *Il4*, and *Il13*) and was best represented by *Il4* based on expression changes. The second configuration showed reduced expression in MA and elevated expression in both old and senescent groups. This configuration contained four genes (*Cxcl13*, *Cd40lg*, *Ccl5*, and *Ccl7*) and was best represented by *Cxcl13*. The third configuration demonstrated a slight decrease or no change in MA, increase in old, and almost returned to baseline levels in senescence. This configuration contained 14 genes and was best represented by *Bcl6*. The fourth configuration was up-regulated in MA and was down-regulated in both old and senescence. This configuration contained 11 genes and was best represented by *Abcf1*. The fifth configuration was up-regulated in MA, down-regulated in old, and returned to baseline levels in senescence. This configuration contained two genes (*Cxcl1* and *Ccl24*) and was best represented by *Ccl24*.

There were two configurations in MMP-9 null mice that defined the cardiac ageing pattern (*Figure 1D*). The first configuration was up-regulated in MA, but down-regulated in the old and senescent group. This configuration included 28 genes and was best represented by *Cxcl10*. The second configuration was reduced in MA, but increased in the old and senescent group. This configuration included seven genes and was best represented by *Crp*. The fact that WT and MMP-9 null configurations were so different indicated a strong reliance of cardiac ageing on MMP-9.

3.3 Inflammatory markers that correlated with chronological ageing

To identify relationships between specific inflammatory markers and cardiac ageing, we performed Pearson correlation analysis to compare gene expression and chronological age for both WT and MMP-9 null groups. There were 43 genes that were $P < 0.05$ and had a correlation coefficient (r) >0.40 or <-0.40 (*Table 2*). Of these, four genes (*Ccl24*, *Il1r1*, *Tollip*, and *Il6st*) showed a similar negative correlation in both WT and MMP-9 null groups. In the WT, *Ccl5*, *Ccl11*, and *Ccl8* showed a strong positive correlation with age, while 13 genes

Table 2 Pearson correlation analysis revealed genes correlated with chronological age in WT or MMP-9 null mice

Gene	WT (r)	MMP-9 null (r)	Effect on inflammation
Both WT and MMP-9 null			
Ccl24	−0.56	−0.41	Pro
Il1r1	−0.50	−0.54	Pro
Tollip	−0.44	−0.42	Anti
Il6st	−0.43	−0.49	Pro
WT			
Ccl5	0.53		Pro
Ccl11	0.53		Pro
Ccl8	0.49		Pro
Bcl6	−0.68		Anti
Ccr10	−0.66		Pro
Ccr8	−0.53		Pro
Tnfrsf1a	−0.52		Pro
Il13	−0.48		Anti
Crp	−0.47		Pro
Il10rb	−0.46		Anti
Il6ra	−0.45		Pro
Il4	−0.42		Anti
MMP-9 null			
Il8rb		0.42	Pro
Cxcl1		−0.79	Pro
Cxcl10		−0.76	Pro
Il2rg		−0.74	Pro
Xcr1		−0.72	Pro
Ccl7		−0.71	Pro
Cxcl9		−0.67	Pro
Ccr5		−0.61	Pro
Ifng		−0.60	Pro
Cx3cl1		−0.59	Pro
Ccl2		−0.58	Pro
Ccr3		−0.55	Pro
Cxcr3		−0.55	Pro
Ccl4		−0.53	Pro
Tgfb1		−0.50	Anti
Ccl3		−0.49	Pro
Il15		−0.49	Pro
Tnf		−0.49	Pro
Ccr6		−0.47	Pro
Il18		−0.46	Pro
Il10ra		−0.45	Anti
Scye1		−0.45	Pro
Ccl17		−0.43	Anti
Cd40lg		−0.43	Pro
Il1f6		−0.42	Pro
Casp1		−0.41	Pro
Itgb2		−0.41	Pro

Out of 84 genes examined, these 43 had a correlation coefficient (r) >0.40 or <-0.40 with $P < 0.05$ for WT or MMP-9 null.

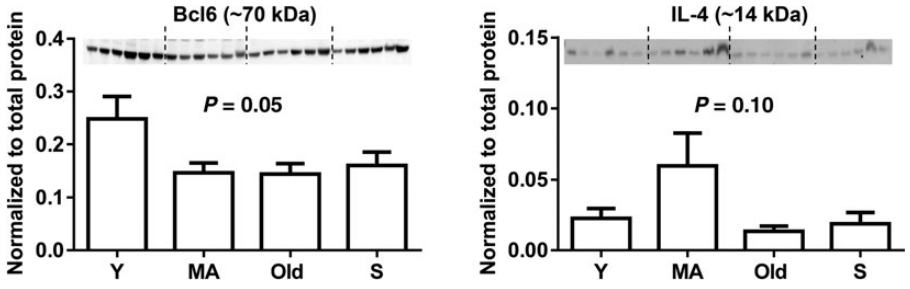

Figure 2 Cardiac protein expression of Bcl6 and IL-4 in young (Y), middle-aged (MA), old, and senescent (S, 26–34 months) WT mice. One-way ANOVA and Sidak's multiple comparisons test were used. $n = 6$/group.

demonstrated a strong negative correlation with age. In the MMP-9 null, only *Il8rb* showed a positive correlation with age, whereas 30 genes demonstrated a negative correlation with age. Interestingly, the majority of the genes that showed a negative correlation with age in the MMP-9 null were pro-inflammatory factors, indicating that MMP-9 deletion facilitated a decrease in pro-inflammatory gene expression. These results also suggested that immunosenescence occurred with cardiac ageing, as a large number of the genes were negatively correlated with age in the WT.

3.4 Cardiac inflammaging signatures

Of the inflammatory genes with potential to serve as cardiac ageing markers, *Bcl6*, *Ccl24*, and *Il4* were shown to be important in the WT by three different analytic approaches (ANOVA, biclustering algorithm, and Pearson correlation), suggesting that these three genes could be candidate inflammaging markers. To determine whether protein levels show a similar change pattern, immunoblotting for two markers was performed for correlation analysis for mRNA and protein (*Figure 2* and see Supplementary material online, *Table S2*). Bcl6 demonstrated a positive correlation between mRNA and protein expression ($r = 0.48$, $P < 0.05$). The mRNA and protein expression of IL-4 did not show significant correlation, which is consistent with past reports of poor correlation between mRNA and protein levels.[22,23] The lack of concordance between mRNA and protein expression may be the result of post-transcriptional regulation or altered protein turnover.

3.5 Distilling the cardiac ageing signature to identify inflammatory markers that predict E/A ratio or LV wall thickness changes with age

We performed correlation analysis between the genes in *Table 1* and E/A ratio or LV wall thickness in diastole (*Table 3*). The *Bcl6*, *Il1r1*, *Ccl24*, and *Crp* genes positively correlated with E/A ratio, but *Cxcl13* negatively correlated with E/A ratio in WT but not in MMP-9 null, indicating that these five gene levels were predictive of E/A ratio. The *Ifng*, *Cxcl1*, *Xcr1*, *Cxcl10*, and *Ccl2* genes showed a positive correlation with E/A ratio in MMP-9 null but not in WT, indicating that these ageing signature markers were MMP-9-dependent. For LV wall thickness, 12 genes (*Abcf1*, *Tollip*, *Scye1*, *Mif*, *Il6st*, *Il16*, *Ccl19*, *Ccr7*, *Il15*, *Spp1*, *Ccr9*, and *Ccr2*) demonstrated a positive correlation in WT. Among those, *Abcf1*, *Tollip*, *Scye1*, and *Mif* had highest correlation coefficient and predicted LV wall changes. In the MMP-9 null, five genes, *Abcf1, Tollip*, *Il6st*, *Il16*, and *Ccr7*, also correlated with wall thickness. *Il1r1* only showed correlation with LV wall thickness in MMP-9 null. This indicated that there was a strong MMP-9 dependence in the relationships between inflammation and LV structure and function.

Table 3 Pearson correlation analysis revealed genes that predict the ratio of early-to-late diastolic filling velocities (E/A ratio) or LV wall thickness changes with chronological age

Genes	WT (*r*)	MMP-9 null (*r*)
E/A ratio associated		
Bcl6	0.69	
Il1r1	0.49	
Ccl24	0.45	
Crp	0.40	
Cxcl13	−0.52	
Ifng		0.61
Cxcl1		0.53
Xcr1		0.53
Cxcl10		0.52
Ccl2		0.46
LV wall thickness associated		
Abcf1	0.70	0.58
Tollip	0.65	0.49
Scye1	0.62	
Mif	0.62	
Il6st	0.61	0.48
Il16	0.60	0.59
Ccl19	0.56	
Ccr7	0.54	0.44
Il15	0.52	
Spp1	0.46	
Ccr9	0.45	
Ccr2	0.42	
Il1r1		0.41

Out of 35 genes examined, these 23 had a correlation coefficient (r) > 0.40 or < -0.40 with $P < 0.05$.

3.6 Macrophage infiltration in the ageing LV was not regulated by MMP-9

To investigate if the differential inflammatory changes in WT and MMP-9 null mice could be attributed to changes in macrophage infiltration,

macrophage numbers in WT and MMP-9 null LV were quantified by immunohistochemical staining. Macrophage numbers significantly increased in the LVs of both WT and MMP-9 null senescent (26–34 months) mice compared with their young controls (*Figure 3A*, both $P < 0.05$). There were no differences in total macrophage numbers between WT and MMP-9 null senescent mice, indicating that the altered inflammatory pattern in the MMP-9 null mice may be due to a difference in macrophage polarization rather than absolute numbers.

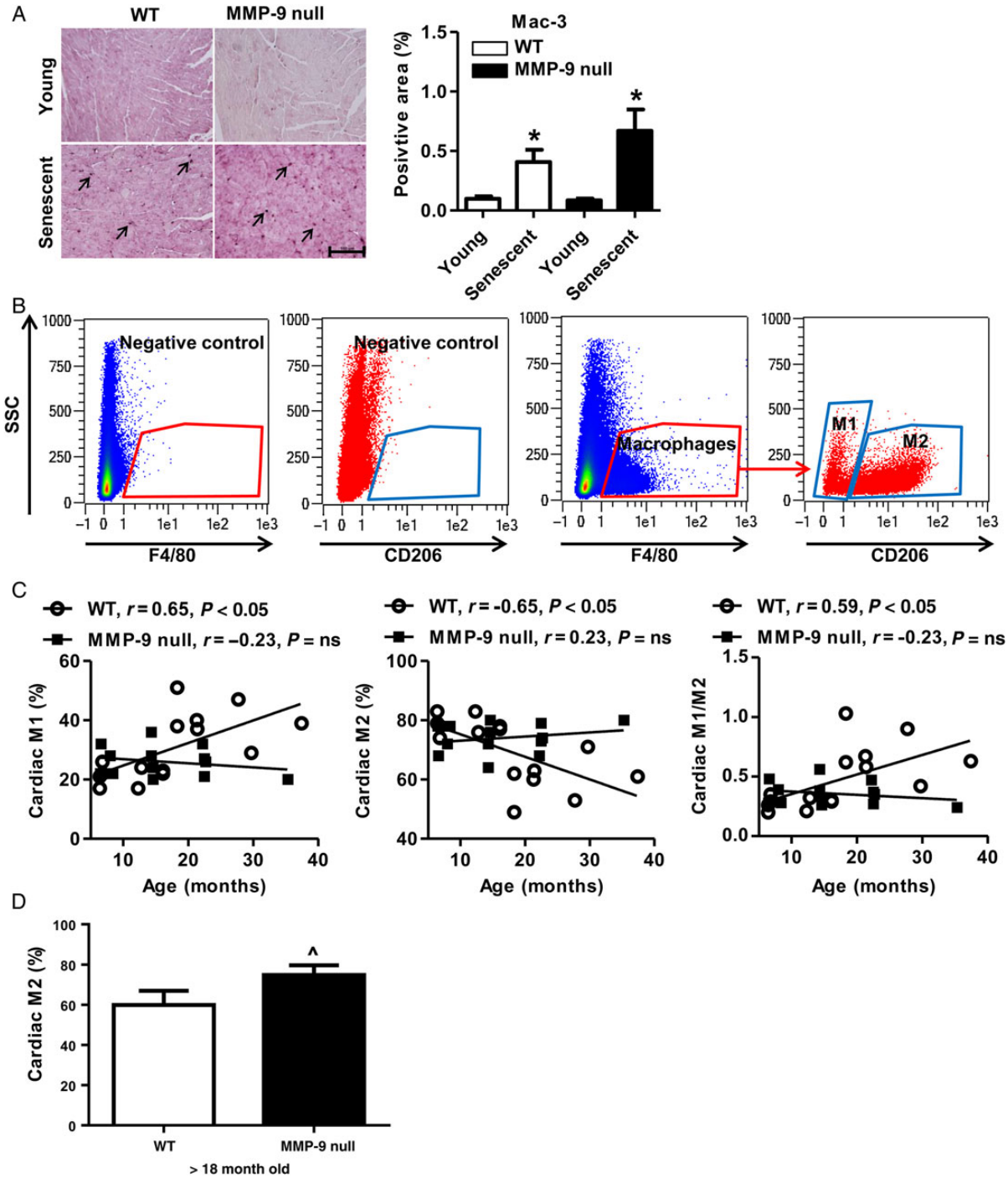

Figure 3 Cardiac macrophage phenotype, but not total number, was regulated by MMP-9 deletion during cardiac ageing. (*A*) Immunohistochemistry for Mac-3 showed a comparable increase in LV macrophage numbers in both WT and MMP-9 null senescent (26–34 months) mice. There were no genotype differences at either age. Positive staining is shown by arrows. Scale bar: 100 μm; $n = 9–13$/group; $^*P < 0.05$ vs. young. (*B*) Representative flow cytometry plots illustrate gating to define macrophages and macrophage M1 and M2 phenotypes. The unstained cells and/or cells stained with isotype-matched IgG were used as negative controls. (*C*) Cardiac M1 macrophages increased while M2 macrophages decreased with age in WT, which were prevented by MMP-9 deletion. Pearson correlation analysis was used. ns, not significant. $n = 13–15$/group. (*D*) MMP-9 null mice (>18 month old) showed a higher percentage of cardiac M2 macrophages than age-matched WT. $n = 5–7$/group. Student's *t*-test was used. Data are represented as mean ± SEM. $^{\wedge}P < 0.05$ vs. WT.

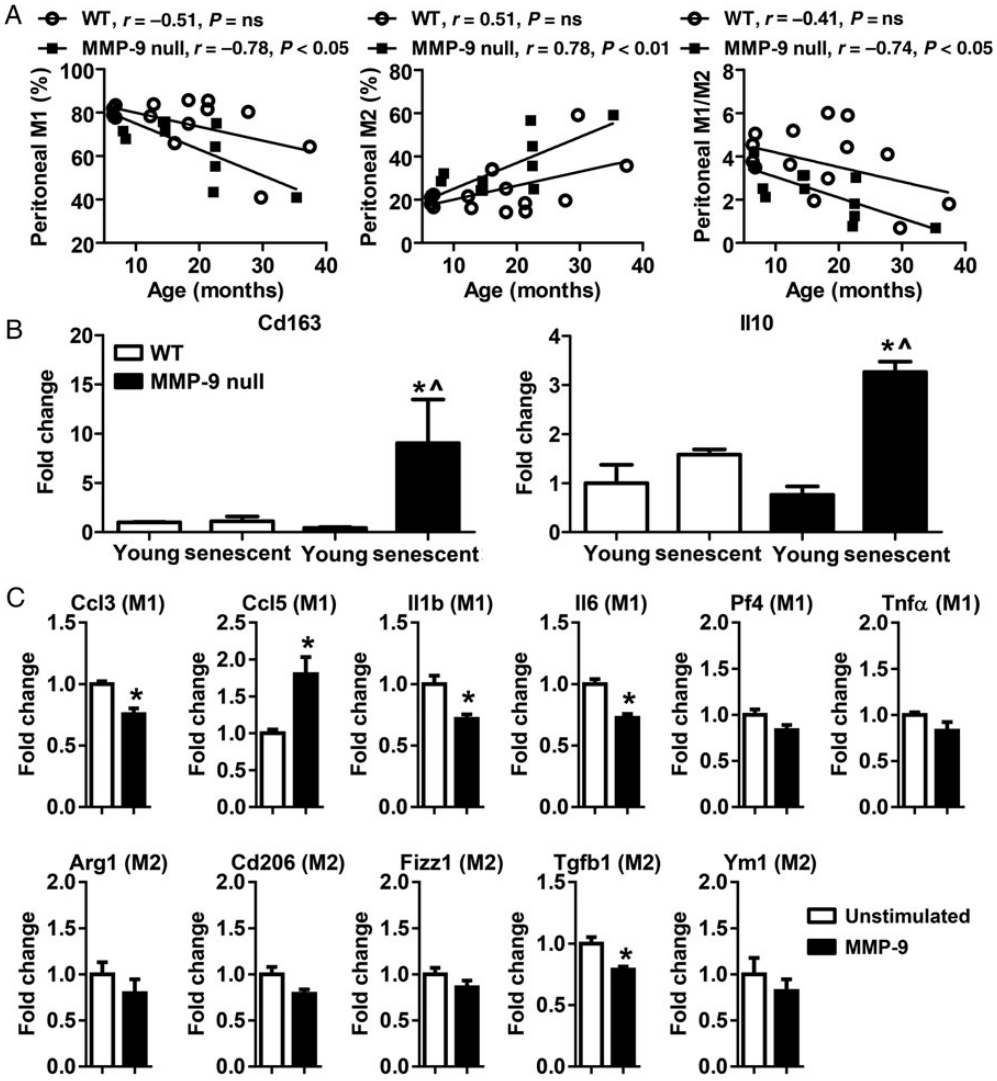

Figure 4 MMP-9 regulates ageing-associated peritoneal macrophage phenotype. (*A*) Peritoneal M1 macrophages decreased while M2 macrophages increased with age in MMP-9 null, but not in WT; ns, not significant; $n = 13–15$/group. Pearson correlation analysis was used. (*B*) The mRNA levels of *Cd163* and *Il10* in peritoneal macrophages of MMP-9 null senescent (26–34 months) mice were higher than MMP-9 null young or WT senescent mice. Two-way ANOVA and Sidak's multiple comparisons test were used; $n = 3–6$/group; $^*P < 0.05$ vs. young and $^\wedge P < 0.05$ vs. WT senescent. (*C*) MMP-9 directly stimulated macrophage activation. MMP-9 stimulation increased the expression of an M1 marker *Ccl5*, but decreased the expression of *Ccl3*, *Il1β*, and *Il6*. *Tgfb1*, an M2 marker, was also down-regulated after MMP-9 treatment. Peritoneal macrophages were isolated from 3- to 6-month-old WT mice. Student's *t*-test was used. Data are represented as mean ± SEM. $n = 4$/group. $^*P < 0.05$ vs. unstimulated.

3.7 MMP-9 deletion regulated cardiac macrophage polarization during cardiac ageing

To determine the effect of ageing and MMP-9 deletion on cardiac macrophage polarization, we assessed cardiac macrophage phenotypes by flow cytometry for young, MA, old, and senescent WT and MMP-9 null LV. As shown in *Figure 3B* and *C*, there was a linear increase with age of M1 macrophages ($F4/80^+CD206^-$) in WT ($P < 0.05$), but not in MMP-9 null. At the same time, there was a linear decrease with age of M2 macrophages ($F4/80^+CD206^+$) in WT ($P < 0.05$), but not in MMP-9 null. This resulted in an increased M1/M2 ratio with age only in WT. We also isolated cardiac macrophages from 18- to 24-month-old mice and measured gene expression profiles of six M1 and four M2 markers by real-time PCR. Compared with WT, MMP-9 null cardiac macrophages showed higher expression of two M2 markers *Cd206* and *Fizz1*; of note, MMP-9 deletion had no significant effect on any of the M1 markers examined (see Supplementary material online, *Figure S1*). Macrophage numbers increased with age, which was not affected by MMP-9 deletion, while there was a higher percentage of cardiac M2 macrophages in the MMP-9 nulls over 18 months of age (*Figure 3D*). Combined, these results indicate higher numbers of M2 macrophages in old MMP-9 null vs. WT. Taken together, pro-inflammatory M1 macrophages increased and anti-inflammatory M2 macrophages decreased during cardiac ageing, and these changes were prevented by MMP-9 deletion. The different macrophage phenotypes observed between WT and MMP-9 null LV with ageing provide a mechanism for the differences in inflammation.

3.8 Regulation of peritoneal macrophage phenotype by MMP-9 deletion

Peritoneal macrophages are commonly used as a surrogate for cardiac macrophages for *in vitro* experiments, due to the lower numbers of cardiac macrophages under normal conditions. We used flow cytometry to evaluate whether peritoneal macrophage phenotype showed a similar pattern with age as cardiac macrophages. As shown in *Figure 4A*, WT peritoneal M1 and M2 macrophages did not correlate with age, which was different from cardiac macrophage phenotype. In contrast, MMP-9 null peritoneal M1 macrophages showed a linear decrease, while M2 macrophages demonstrated a linear increase with age, which resulted in a reduced M1/M2 ratio due to this switch in phenotype. Therefore, MMP-9 deletion down-regulated ageing-associated peritoneal M1 macrophages but up-regulated M2 macrophages. That cardiac and peritoneal macrophages show different phenotypic changes with ageing indicates that macrophages respond to ageing based on their location and origin of source.[24]

Next, we compared the mRNA expression levels of M2 markers in peritoneal macrophages isolated from young and senescent (26–34 months) WT and MMP-9 null mice. Macrophages from MMP-9 null senescent showed higher expression of M2 markers *Cd163* and *Il10*, compared with young MMP-9 null and senescent WT controls (*Figure 4B*, both $P < 0.05$). These findings consistently indicated that MMP-9 deletion enhanced ageing-associated peritoneal macrophage polarization to an M2 subtype in the senescent cells.

3.9 MMP-9 directly activates macrophage polarization to an M1/M2 transition phenotype

To rule out that the MMP-9 effect was indirect through regulation of cytokines and chemokines, we directly stimulated young (3–6 month old) peritoneal macrophages with recombinant MMP-9 protein. We measured gene expression of six M1 and five M2 markers (*Figure 4C*). Of those, three M1 markers (*Ccl3*, *Il1b*, and *Il6*) and an M2 marker *Tgfb1* were down-regulated; in contrast, M1 marker *Ccl5* was up-regulated after MMP-9 treatment. Combined, these results indicate that MMP-9 stimulates a transition phenotype that is neither entirely M1 nor entirely M2. This reveals specific pathways that are directly influenced by MMP-9. To investigate whether MMP-9 has similar stimulatory roles on the polarization of old macrophages, we isolated peritoneal macrophages from 18- to 24-month-old WT mice and stimulated them with MMP-9. Interestingly, MMP-9 treatment had no significant effect on the expression of the same M1 and M2 markers examined in the young, indicating that ageing desensitized peritoneal macrophages to MMP-9 *in vitro* (see Supplementary material online, *Figure S2*). Further experiments are needed to determine whether undefined systemic changes *in vivo* are required for MMP-9-induced macrophage polarization particularly in aged mice.

4. Discussion

This study established the cardiac ageing biological inflammatory signature and defined MMP-9 regulation of this signature. The principal findings were that, for cardiac ageing: (i) *Bcl6*, *Ccl24*, and *Il4* were the strongest inflammatory markers of the cardiac ageing signature; (ii) *Bcl6*, *Il1r1*, *Ccl24*, *Crp*, and *Cxcl13* predicted E/A ratio changes while *Abcf1*, *Tollip*, *Scye1*, and *Mif* predicted LV wall thickness changes; (iii) MMP-9 deletion did not influence LV macrophage numbers, but stimulated macrophage polarization to the M2 phenotype; and (iv) cardiac and peritoneal macrophages showed distinct phenotypic changes with ageing. This is the first report that defines the biological ageing signature, to distinguish from chronological ageing patterns, and connects the biological ageing signature to LV structure and function based on MMP-9 effects on macrophage polarization.

Bcl6, one of the most significant genes in the pattern, is a transcriptional repressor with anti-apoptotic and pro-oncogenic properties.[25] A recent study by Chen *et al.*[26] revealed that Bcl6 expression was down-regulated in senescent fibroblasts compared with young fibroblasts, indicating that the senescence process involved reduced Bcl6. In line with the above findings, our study found that senescent hearts showed reduced Bcl6 expression compared with young mice. Analysis of the gene array and protein data by multiple approaches confirmed that the loss of Bcl6 is a promising ageing marker.

Ccl24, also known as myeloid progenitor inhibitory factor 2 (MPIF-2) or eosinophil chemotactic protein 2 (eotaxin-2), belongs to the CC chemokine family. CCl24 is a chemotactic for neutrophils and T lymphocytes.[27] Here we, for the first time, reported that CCl24 might serve as a potential candidate marker for cardiac ageing based on our bioinformatics analysis. Further experiments are needed to elucidate the role of Ccl24 in cardiac ageing.

IL-4 is a classic anti-inflammatory mediator. IL-4 has recently been reported to induce senescence in human renal carcinoma cell lines via STAT6 and p38 MAPK signalling pathways.[28] Our data demonstrated that IL-4 was down-regulated in the MA pattern and continuously up-regulated from the MA to senescent patterns. Of note, Bcl6 was shown to negatively modulate STAT-dependent IL-4 signalling.[29] This could explain our results showing opposite patterns in Bcl6 and IL-4 expression in the middle age pattern.

The E/A ratio, a cardiac diastolic function variable, is impaired with chronological ageing and this impairment is protected by MMP-9 deletion.[5] In this study, we demonstrated that *Bcl6*, *Il1r1*, *Ccl24*, *Crp*, and *Cxcl13* positively correlated with E/A ratio, and *Abcf1*, *Tollip*, *Scye1*, and *Mif* positively correlated with LV wall thickness. These data indicated that these genes could serve as markers for predicting E/A ratio or LV wall thickness in the aged mice.

We previously evaluated neutrophil infiltration in cardiac ageing.[5] Neutrophil infiltration did not significantly change with age in both WT and MMP-9 null mice. Therefore, the major cellular source of the inflammatory proteins in the ageing heart is likely from infiltrated macrophages. Macrophages play a pivotal role in cardiovascular disease, such as atherosclerosis, myocardial infarction, and heart failure.[30] We noted low macrophage numbers in our young mice. A recent study by Eric Olson's group reported high numbers of resident cardiac macrophages in neonate mouse, indicating that macrophage numbers decline during maturation to adult.[31] Dr Ungvari's group demonstrated that ageing significantly increased macrophage infiltration in periaortic adipose tissue, which elevated the risk for the development of cardiovascular diseases in the elderly population.[32] Both this study and our previous work demonstrated that macrophage numbers in the LV increased with age, which produce more MMP-9 and facilitate cardiac ageing.[5] While MMP-9 deletion has been shown to reduce macrophage infiltration post-MI, MMP-9 deletion did not regulate macrophage infiltration during ageing.[12] This finding raises the possibility that MMP-9 deletion effects on ageing inflammation may be due more to the regulation of macrophage polarization.[33,34]

A broad but likely oversimplified macrophage classification is the classical M1 and alternative M2 subtypes.[35] M1 macrophages are

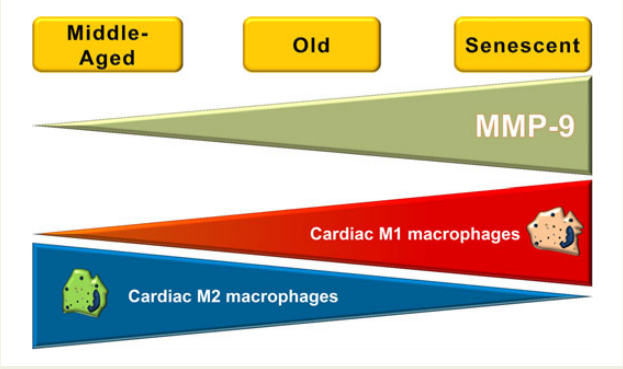

Figure 5 Inflammatory mechanisms of cardiac ageing. A schematic summary of our results shows that, as MMP-9 increases with age, cardiac pro-inflammatory M1 macrophages also increase, while anti-inflammatory M2 macrophages decrease. MMP-9 deletion prevented the increase in M1 and decrease in M2, with the overall effect being to preserve cardiac function for a longer period of time.

pro-inflammatory and facilitate extracellular matrix degradation, whereas M2 macrophages are anti-inflammatory and promote post-injury repair and wound healing.[16,36,37] A recent study revealed that cardiac macrophage phenotype changes with age, and age-related changes in cardiac tissue macrophages precede cardiac functional impairment.[38] In the WT, ageing induced M1 macrophage activation. Both Pearson correlation analysis and real-time PCR experiments confirmed that MMP-9 deletion prevented M1 polarization and stimulated M2 activation during the cardiac ageing process. Our flow cytometry data also confirmed that cardiac M1 macrophages increased while M2 macrophages decreased with age, which was prevented by MMP-9 deficiency. In addition, our *in vitro* experiments revealed that MMP-9 directly stimulated peritoneal macrophage polarization to a transition phenotype that was part M1 and part M2, as evidenced by altered expression levels of both M1 and M2 markers. Our results suggest that, during cardiac ageing, MMP-9 may coordinate the switch in macrophage phenotype by unknown indirect mechanisms. Cardiac and peritoneal macrophages showed distinct phenotypic changes with ageing. Investigating the underlying mechanisms whereby cardiac and peritoneal macrophage phenotypes differentially alter with age may provide further insights.

Our study revealed that the cardiac ageing inflammatory markers could predict cardiac structural and functional changes, and MMP-9 deletion can attenuate ageing-associated cardiac fibrosis and diastolic dysfunction by mediating the inflammatory response to ageing. In conclusion, (i) ageing induced macrophage accumulation in the LV, which leads to more MMP-9.[5] MMP-9, in turn, facilitated cardiac ageing and inflammaging by regulating macrophage polarization and (ii) MMP-9 deletion modulated the ageing signature by preventing ageing-associated M1 macrophage polarization and facilitating M2 macrophage polarization, resulting in attenuated collagen deposition and LV diastolic dysfunction (*Figure 5*).

Supplementary material

Supplementary material is available at *Cardiovascular Research* online.

Acknowledgements

We thank Trevi A. Ramirez and Jianhua Zhang for technical assistance.

Conflict of interest: none declared.

Funding

This work was supported by American Heart Association Scientist Development Grant (15SDG22930009 to Y.M.); the National Institutes of Health [HHSN 268201000036C (N01-HV-00244) and HL075360 to M.L.L., P01HL051971, P20GM104357]; and the Biomedical Laboratory Research and Development Service of the Veterans Affairs Office of Research and Development Award (5I01BX000505 to M.L.L.).

References

1. Boon RA, Iekushi K, Lechner S, Seeger T, Fischer A, Heydt S, Kaluza D, Treguer K, Carmona G, Bonauer A, Horrevoets AJ, Didier N, Girmatsion Z, Biliczki P, Ehrlich JR, Katus HA, Muller OJ, Potente M, Zeiher AM, Hermeking H, Dimmeler S. MicroRNA-34a regulates cardiac ageing and function. *Nature* 2013;**495**:107–110.
2. Jackson SH, Weale MR, Weale RA. Biological age—what is it and can it be measured? *Arch Gerontol Geriatr* 2003;**36**:103–115.
3. Lin J, Lopez EF, Jin Y, Van Remmen H, Bauch T, Han HC, Lindsey ML. Age-related cardiac muscle sarcopenia: combining experimental and mathematical modeling to identify mechanisms. *Exp Gerontol* 2008;**43**:296–306.
4. Dutta D, Calvani R, Bernabei R, Leeuwenburgh C, Marzetti E. Contribution of impaired mitochondrial autophagy to cardiac aging: mechanisms and therapeutic opportunities. *Circ Res* 2012;**110**:1125–1138.
5. Chiao YA, Ramirez TA, Zamilpa R, Okoronkwo SM, Dai Q, Zhang J, Jin YF, Lindsey ML. Matrix metalloproteinase-9 deletion attenuates myocardial fibrosis and diastolic dysfunction in ageing mice. *Cardiovasc Res* 2012;**96**:444–455.
6. Baylis D, Bartlett DB, Patel HP, Roberts HC. Understanding how we age: insights into inflammaging. *Longev Healthspan* 2013;**2**:8.
7. Chiao YA, Dai Q, Zhang J, Lin J, Lopez EF, Ahuja SS, Chou YM, Lindsey ML, Jin YF. Multi-analyte profiling reveals matrix metalloproteinase-9 and monocyte chemotactic protein-1 as plasma biomarkers of cardiac aging. *Circ Cardiovasc Genet* 2011;**4**:455–462.
8. Xia Y, Frangogiannis NG. MCP-1/CCL2 as a therapeutic target in myocardial infarction and ischemic cardiomyopathy. *Inflamm Allergy Drug Targets* 2007;**6**:101–107.
9. Han L, Li M, Liu Y, Han C, Ye P. Atorvastatin may delay cardiac aging by upregulating peroxisome proliferator-activated receptors in rats. *Pharmacology* 2012;**89**:74–82.
10. Mercken EM, Crosby SD, Lamming DW, JeBailey L, Krzysik-Walker S, Villareal DT, Capri M, Franceschi C, Zhang Y, Becker K, Sabatini DM, de Cabo R, Fontana L. Calorie restriction in humans inhibits the PI3K/AKT pathway and induces a younger transcription profile. *Aging Cell* 2013;**12**:645–651.
11. Lindsey ML, Escobar GP, Dobrucki LW, Goshorn DK, Bouges S, Mingoia JT, McClister DM Jr, Su H, Gannon J, MacGillivray C, Lee RT, Sinusas AJ, Spinale FG. Matrix metalloproteinase-9 gene deletion facilitates angiogenesis after myocardial infarction. *Am J Physiol Heart Circ Physiol* 2006;**290**:H232–H239.
12. Ducharme A, Frantz S, Aikawa M, Rabkin E, Lindsey M, Rohde LE, Schoen FJ, Kelly RA, Werb Z, Libby P, Lee RT. Targeted deletion of matrix metalloproteinase-9 attenuates left ventricular enlargement and collagen accumulation after experimental myocardial infarction. *J Clin Invest* 2000;**106**:55–62.
13. Yabluchanskiy A, Ma Y, Chiao YA, Lopez EF, Voorhees AP, Toba H, Hall ME, Han HC, Lindsey ML, Jin YF. Cardiac aging is initiated by matrix metalloproteinase-9 mediated endothelial dysfunction. *Am J Physiol Heart Circ Physiol* 2014;**306**:H1398–H1407.
14. Vu TH, Shipley JM, Bergers G, Berger JE, Helms JA, Hanahan D, Shapiro SD, Senior RM, Werb Z. MMP-9/gelatinase B is a key regulator of growth plate angiogenesis and apoptosis of hypertrophic chondrocytes. *Cell* 1998;**93**:411–422.
15. Martin MD, Carter KJ, Jean-Philippe SR, Chang M, Mobashery S, Thiolloy S, Lynch CC, Matrisian LM, Fingleton B. Effect of ablation or inhibition of stromal matrix metalloproteinase-9 on lung metastasis in a breast cancer model is dependent on genetic background. *Cancer Res* 2008;**68**:6251–6259.
16. Ma Y, Halade GV, Zhang J, Ramirez TA, Levin D, Voorhees A, Jin YF, Han HC, Manicone AM, Lindsey ML. Matrix metalloproteinase-28 deletion exacerbates cardiac dysfunction and rupture after myocardial infarction in mice by inhibiting m2 macrophage activation. *Circ Res* 2013;**112**:675–688.
17. Bustin SA, Benes V, Garson JA, Hellemans J, Huggett J, Kubista M, Mueller R, Nolan T, Pfaffl MW, Shipley GL, Vandesompele J, Wittwer CT. The MIQE guidelines: minimum information for publication of quantitative real-time PCR experiments. *Clin Chem* 2009;**55**:611–622.
18. Ghasemi O, Nguyen N, Ramirez TA, Zhang J, Lindsey ML, Jin Y-F. A biclustering approach to analyze drug effects on extracellular matrix remodeling post-myocardial infarction. In *2012 IEEE International Conference on Bioinformatics and Biomedicine Workshops (BIBMW 2012)*. Philadelphia, USA: ; 2012. p. 143–150.
19. Ma Y, Chiao YA, Zhang J, Manicone AM, Jin YF, Lindsey ML. Matrix metalloproteinase-28 deletion amplifies inflammatory and extracellular matrix responses to cardiac aging. *Microsc Microanal* 2012;**18**:81–90.
20. Zamilpa R, Ibarra J, de Castro Bras LE, Ramirez TA, Nguyen N, Halade GV, Zhang J, Dai Q, Dayah T, Chiao YA, Lowell W, Ahuja SS, D'Armiento J, Jin YF, Lindsey ML. Transgenic overexpression of matrix metalloproteinase-9 in macrophages attenuates the

inflammatory response and improves left ventricular function post-myocardial infarction. *J Mol Cell Cardiol* 2012;**53**:599–608.
21. Yan X, Anzai A, Katsumata Y, Matsuhashi T, Ito K, Endo J, Yamamoto T, Takeshima A, Shinmura K, Shen W, Fukuda K, Sano M. Temporal dynamics of cardiac immune cell accumulation following acute myocardial infarction. *J Mol Cell Cardiol* 2013;**62**:24–35.
22. Shebl FM, Pinto LA, Garcia-Pineres A, Lempicki R, Williams M, Harro C, Hildesheim A. Comparison of mRNA and protein measures of cytokines following vaccination with human papillomavirus-16 L1 virus-like particles. *Cancer Epidemiol Biomarkers Prev* 2010;**19**:978–981.
23. Schwanhausser B, Busse D, Li N, Dittmar G, Schuchhardt J, Wolf J, Chen W, Selbach M. Global quantification of mammalian gene expression control. *Nature* 2011;**473**:337–342.
24. Heidt T, Courties G, Dutta P, Sager HB, Sebas M, Iwamoto Y, Sun Y, Da Silva N, Panizzi P, van der Lahn AM, Swirski FK, Weissleder R, Nahrendorf M. Differential contribution of monocytes to heart macrophages in steady-state and after myocardial infarction. *Circ Res* 2014;**115**:284–295.
25. Saito Y, Liang G, Egger G, Friedman JM, Chuang JC, Coetzee GA, Jones PA. Specific activation of microRNA-127 with downregulation of the proto-oncogene BCL6 by chromatin-modifying drugs in human cancer cells. *Cancer Cell* 2006;**9**:435–443.
26. Chen J, Wang M, Guo M, Xie Y, Cong YS. miR-127 regulates cell proliferation and senescence by targeting BCL6. *PLoS ONE* 2013;**8**:e80266.
27. Patel VP, Kreider BL, Li Y, Li H, Leung K, Salcedo T, Nardelli B, Pippalla V, Gentz S, Thotakura R, Parmelee D, Gentz R, Garotta G. Molecular and functional characterization of two novel human C-C chemokines as inhibitors of two distinct classes of myeloid progenitors. *J Exp Med* 1997;**185**:1163–1172.
28. Kim HD, Yu SJ, Kim HS, Kim YJ, Choe JM, Park YG, Kim J, Sohn J. Interleukin-4 induces senescence in human renal carcinoma cell lines through STAT6 and p38 MAPK. *J Biol Chem* 2013;**288**:28743–28754.
29. Hartatik T, Okada S, Okabe S, Arima M, Hatano M, Tokuhisa T. Binding of BAZF and Bc16 to STAT6-binding DNA sequences. *Biochem Biophys Res Commun* 2001;**284**:26–32.
30. Swirski FK, Nahrendorf M. Leukocyte behavior in atherosclerosis, myocardial infarction, and heart failure. *Science* 2013;**339**:161–166.
31. Aurora AB, Porrello ER, Tan W, Mahmoud AI, Hill JA, Bassel-Duby R, Sadek HA, Olson EN. Macrophages are required for neonatal heart regeneration. *J Clin Invest* 2014;**124**:1382–1392.
32. Bailey-Downs LC, Tucsek Z, Toth P, Sosnowska D, Gautam T, Sonntag WE, Csiszar A, Ungvari Z. Aging exacerbates obesity-induced oxidative stress and inflammation in perivascular adipose tissue in mice: a paracrine mechanism contributing to vascular redox dysregulation and inflammation. *J Gerontol A Biol Sci Med Sci* 2013;**68**:780–792.
33. Biswas SK, Chittezhath M, Shalova IN, Lim JY. Macrophage polarization and plasticity in health and disease. *Immunol Res* 2012;**53**:11–24.
34. Nahrendorf M. Macrophages in the infarct: fiery friends or friendly fire? *J Mol Cell Cardiol* 2012;**53**:591–592.
35. Mosser DM, Edwards JP. Exploring the full spectrum of macrophage activation. *Nat Rev Immunol* 2008;**8**:958–969.
36. Brown BN, Ratner BD, Goodman SB, Amar S, Badylak SF. Macrophage polarization: an opportunity for improved outcomes in biomaterials and regenerative medicine. *Biomaterials* 2012;**33**:3792–3802.
37. Marchetti V, Yanes O, Aguilar E, Wang M, Friedlander D, Moreno S, Storm K, Zhan M, Naccache S, Nemerow G, Siuzdak G, Friedlander M. Differential macrophage polarization promotes tissue remodeling and repair in a model of ischemic retinopathy. *Sci Rep* 2011;**1**:76.
38. Pinto AR, Godwin JW, Chandran A, Hersey L, Ilinykh A, Debuque R, Wang L, Rosenthal NA. Age-related changes in tissue macrophages precede cardiac functional impairment. *Aging (Albany NY)* 2014;**6**:399–413.